Failure Detection by Signal Similarity Measurement of Brushless DC Motors

Vito Mario Fico [1,*], **Antonio Leopoldo Rodríguez Vázquez** [1], **María Ángeles Martín Prats** [2] **and Franco Bernelli-Zazzera** [3]

[1] Skylife Engineering, 41092 Seville, Spain; antoniorv@skylife-eng.com
[2] Escuela Técnica Superior de Ingeniería, Electronics Engineering Department, Universidad de Sevilla, 41092 Seville, Spain; mmprats@us.es
[3] Department of Aerospace Science and Technology, Politecnico di Milano, 20156 Milan, Italy; franco.bernelli@polimi.it
[*] Correspondence: vito.fico@skylife-eng.com

Abstract: In recent years, Brushless DC (BLDC) motors have been gaining popularity as a solution for providing mechanical power, starting from low cost mobility solutions like the electric bikes, to high performance and high reliability aeronautical Electro-Mechanical Actuator (EMA). In this framework, the availability of fault detection tools suited to these types of machines appears necessary. There is already a vast literature on this topic, but only a small percentage of the proposed techniques have been developed to a sufficiently high Technology Readiness Level (TRL) to be implementable in industrial applications. The investigation on the state of the art carried out during the first phase of the present work, tried to collect the techniques which are closest to possible implementation. To fill a gap identified in the current techniques, a partial demagnetisation detection method is proposed in this paper. This technique takes advantage of the asymmetries generated in the current by the missing magnetic flux to detect the failure. Simulations and laboratory experiments have been carried out to validate the idea, showing the potential and the easy implementation of the method. The results have been examined in detail and satisfactory conclusions have been drawn.

Keywords: failure; PMSM; detection; diagnosis; BLDC; brushless; phase voltage similarity

1. Introduction

With the increasing dependence on electrical devices, condition monitoring of electrical machines is becoming increasingly important, in particular when aerospace applications are involved, since safety becomes one key design driver.

Performance of flight actuators on a damaged aircraft is not as important as ensuring that the remaining actuators continue in operation until the aircraft can land safely. An adequate level of reliability can be reached only by using diagnostic tools. The term diagnosis indicates the process of determining by examination the nature and circumstances of a non-nominal condition. It can be performed collecting information provided by on-line sensors and extracting from them the characteristics that show the current condition of equipment or a process.

This instrument has great importance because an accurate and efficient means of condition monitoring and machine fault diagnosis can drastically improve reliability and stability of the plant as well as reducing costs, leading to a system with virtually no need for programmed maintenance. Statistical studies show that expected reliability can be improved by up to 5–6 percentage points with the use of monitoring [1]. An ideal diagnostic procedure should take the minimum measurements

necessary from a machine and by analysis, extract a diagnosis, so that its condition can be inferred to give a clear indication of incipient failure modes in the minimum time.

Before developing monitoring techniques, several studies must be carried out to understand the failure mechanism in an electrical machine. Broadly, the failure in electrical machine could be classified as electrical or mechanical in nature depending upon the root cause of failures. To characterise the nature of the failure in electrical machines, suitable signature acquisition and processing are required. Noninvasive monitoring is achieved by relying on easily measured electrical or mechanical quantities, such as current, voltage, flux, torque, and speed. The reliable identification and isolation of faults is still, however, under investigation as there are some current issues [2]:

- Definition of a single diagnostic procedure for identification and isolation of any type of faults
- Insensitivity to operating conditions
- Reliable fault detection for position, speed and torque controlled drives
- Reliable fault detection for drives in time-varying conditions
- Quantitative fault detection in order to state an absolute fault threshold, independent of operating conditions

The first step in a research work is certainly the literature review, created in order to understand not only the current state of affairs, but also the evolution. In the field of engineering, and in particular for aerospace engineering, traditional (or narrative) revision is preferred, in which the authors decide the papers to be included in the review based on their deep knowledge and experience and giving a personal vision and interpretation of the topic. The systematic literature review (Systematic Literature Review (SLR)) is a very rigorous and reliable standardised scientific methodology, mainly characterised by its objectivity. This is used with excellent results in many areas, including psychology, medicine and in recent years also in software engineering. In this paper, a SLR on high TRL fault detection techniques for Brushless DC (BLDC) motors is presented. The guidelines presented in [3] for software engineering and [4] for systems and automation engineering have been taken into account; in particular from the latter many ideas and suggestions have been followed when using and evaluating the protocol.

The aim of this review is to indicate which techniques are currently being used successfully for motor fault detection and diagnosis, also to provide the industry with tested techniques and a high level of preparedness. In this view, many of the inclusion (Table 1) and exclusion criteria (Table 2) have been formulated to focus the research on those techniques with demonstrated failure detection performance at various operational points and can be easily automatable or is already automated.

In particular, PhD theses have been excluded because they do not pass under a peer review process. Another reason is that normally, the PhD theses result in one or more papers.

Another important point considered in the review has been the possibility to embed the hardware needed for fault detection within the body of the motor. Indeed, although most papers focused on the detection by using variables already measured (current, voltage and speed) some authors developed failure detection techniques by analysing images from external cameras or very sensitive (and bulky) accelerometers. These techniques are suitable to be implemented only in very particular applications.

2746 papers were initially selected and a first screening to eliminate the duplicates allowed the deletion of 1111 papers from the list; this was due to the fact that many databases share the same publishers. Once the duplicates had been removed, it was necessary to eliminate the grey literature (reviews, books, PhD theses) as it was not possible to exclude it during the research for some databases.

The following step consists in reading the title, abstracts and keywords and in applying the inclusion and exclusion criteria to the remaining 1635 articles. Often, by only reading these fields it was not clear whether the article met all the specified requirements or not, so it was necessary to read the whole article. This problem is mainly due to the fact that in the field of engineering in general, there is no normalisation of rules to create these fields, as exists in other sectors such as medicine or psychology.

Table 1. Inclusion Criteria.

Num.	Description
1	Will propose at least one detection technique (a parameter or an index that clearly and uniquely identifies the failure or an automatic detection algorithm).
2	The proposed technique should not be restricted to a particular machine type (number of phases, etc.).
3	To be applied the technique will not need special equipment, configurations, loads or motor operation.
4	The technique shall have been tested at various operation points (different speed or loads or a combination of both)
5	Characteristics of the detection and diagnosis algorithm: a. The algorithm (or index) will have been tested with success for at least one of the following cases: • Different levels of the same failure, demonstrating coherence (whether by simulation or test on real motor) • On different real motors, demonstrating coherence • On simulation and then real on a motor, demonstrating coherence • Capability to discern between different types of failure b. The paper shall demonstrate that the algorithm is capable to discern between healthy and faulty

Table 2. Exclusion Criteria.

Num.	Description
1	Grey literature and secondary studies (reviews, books, PhD theses)
2	Non English written papers
3	Duplicated studies
4	Full paper not available
5	Does not present tests or simulations
6	Uses big sensors, which cannot be embedded in the motor (such as cameras or similar)
7	Does not concentrate on the topic

In conclusion, from the total set of papers, 307 of have been accepted for full paper review and finally, only 37 papers met the selected criteria for being included in the revision.

In the following subsection the synthesis of such research is reported. It considers statistical data of the distribution of failures, failure detection techniques and more in general about the chosen topic.

1.1. Discussion

A considerable amount of papers (1635) has been found by consulting several databases adopting the aforementioned inclusion and exclusion criteria. The research community is very interested in this topic and the interest has been growing very rapidly over the last few years. Figure 1 shows this trend by representing the number of papers per year published on this topic (results from 1990 to 2017) emerged from the research and after the first screening has been passed.

The trend is probably due to the recent surge in developing high reliability electric vehicles and aircraft, but also to the availability of new techniques and more powerful processors which paved the way to innovative applications.

In this view it is interesting to see how the number of papers based on certain techniques according to the year of publication is distributed (Figure 2).
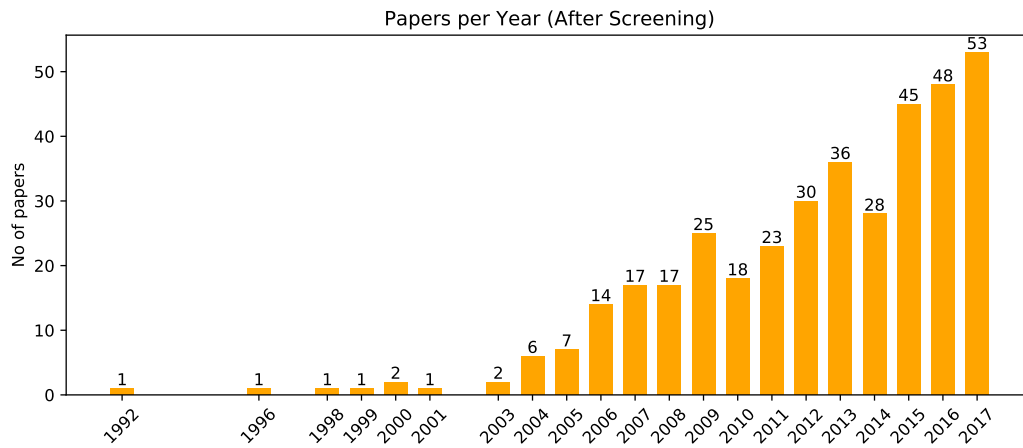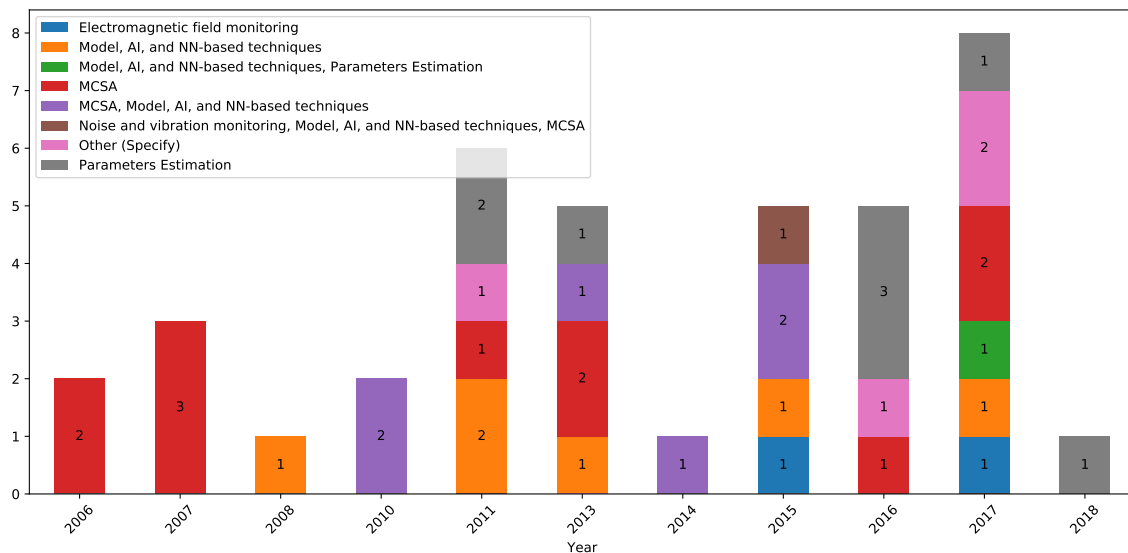
Figure 1. Distribution of papers per Year.

Figure 2. Distribution of the used techniques over the publication year.

Even if the graph in Figure 2 is not representative of the entire literature, it is possible to draw some conclusions. First of all, it appears evident that during recent years the techniques based on models, parameters estimation and Artificial Intelligence (AI) are being used increasingly, often in conjunction with more established methods like the Motor Current Signature Analysis (MCSA) as classifiers.

Also the number of papers discussing techniques based on MCSA has drastically reduced, probably because this is an already been a very well studied technique. The graph in Figure 3 shows the overall distribution of the papers according to the technique used.

The MCSA is still the most used technique, followed by the AI algorithms and the techniques based on parameter estimation. It has to be said that often the techniques based on AI and Neural Network (NN) are used just as classificators in conjunction with other, already established, methods for failure detection. This association has been demonstrated to be of great help in improving the detection rate and extending the use of the technique for a wider range of speeds and loads.

Another important aspect is the presence of a good portion of papers discussing techniques not previously classified and grouped under the tag other. Among them it is possible to find innovative techniques based on High Frequency (HF) Injection [5] or hall effect sensors measurements [6].

Based on the selected papers, the state of the art of BLDC motors fault detection can be outlined as below.
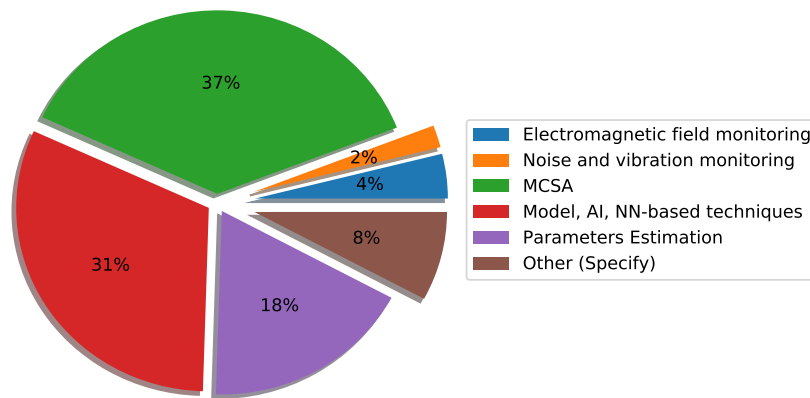
Figure 3. Distribution of the papers according to the technique used.

1.1.1. Most Common Failures of BLDC Motors

Figure 4 shows the distribution of the papers in relation to the type of failure discussed. The results are in accordance with the failure distribution presented in various papers [7–10], and, in turn, this means that the research efforts are consistent with the most common diffuse failures.
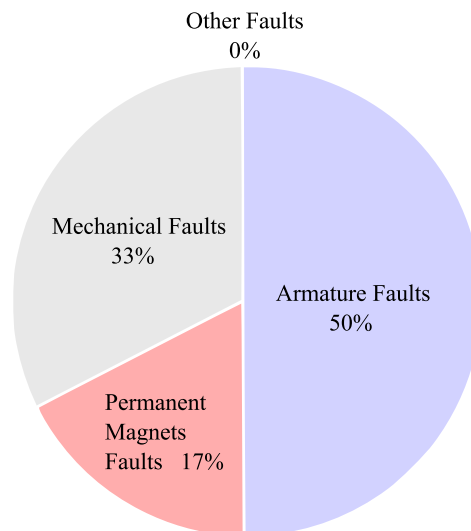

Figure 4. Distribution of the papers according the type of failure examined.

1.1.2. Parameters Used for Fault Detection in BLDC Motors

Almost every physical quantity of the motor can be used to detect eventual failures. In the following, the variables used will be listed, dividing them between those directly measurable and those estimated.

Directly Measurable Quantities: The quantities listed below are directly measurable by the use of sensors.

Current In the majority of cases the current is already measured by the motor controller and there exist a huge quantity of failure detection algorithms based on this variable.

Voltage The voltage also is often already measured by the motor controller. It can be used to extract the back-ElectroMotive Force (EMF).

Vibrations The motor vibration level is detected by mean of accelerometers, which need to be placed close to the item to be monitored. The algorithms based on vibrations analysis could present problems when used in moving systems, like aircraft, due to the coupling of external and unpredictable vibrations.

Output Torque The output torque is measured with torque-meters and can provide very useful information, but this type of sensors are often big and expensive and are maybe better suited for critical applications.

Magnetic Flux The magnetic flux can give a deep insight on how the motor is working. In order to be measured it, it is necessary to include in the motor winding so called search coils, i.e., some additional windings not connected to the phases. The inclusion of these additional coils is not common and, although being a simple procedure, it necessitates the motor to be opened and rewound and to extract from the interior pairs of wires for as many search coils as are inserted.

Estimated Quantities: The techniques based on parameters estimation can detect failures by estimating the changes in the measured motor parameters as well as quantifying variables which are not directly measurable, such as:

- Winding resistance,
- Winding inductance,
- Back-EMF,
- Magnetic flux.

Estimation is a powerful tool which permits the use of variables directly related to the fault and otherwise not measurable, but it depends on models which could be limited to specific situations and on different parameters which might vary.

1.1.3. Type of Failures Detectable by Each Technique

Figure 5 shows the various techniques proposed for the detection of different types of failure. Multiple failures have also been included, in order to evaluate which techniques are most suited to detect and distinguish between different types of failure. This graph is also intended to discover if certain techniques are more suited to detect any particular failure or can be used as a wide spectrum analysis tool.

The techniques are well distributed among the failure types and the main methods appear to be used to detect both individual and multiple failures. Only vibration monitoring appears limited to mechanical fault detection, but this fact can be biased due to the presence in the review of only a single paper in this category.
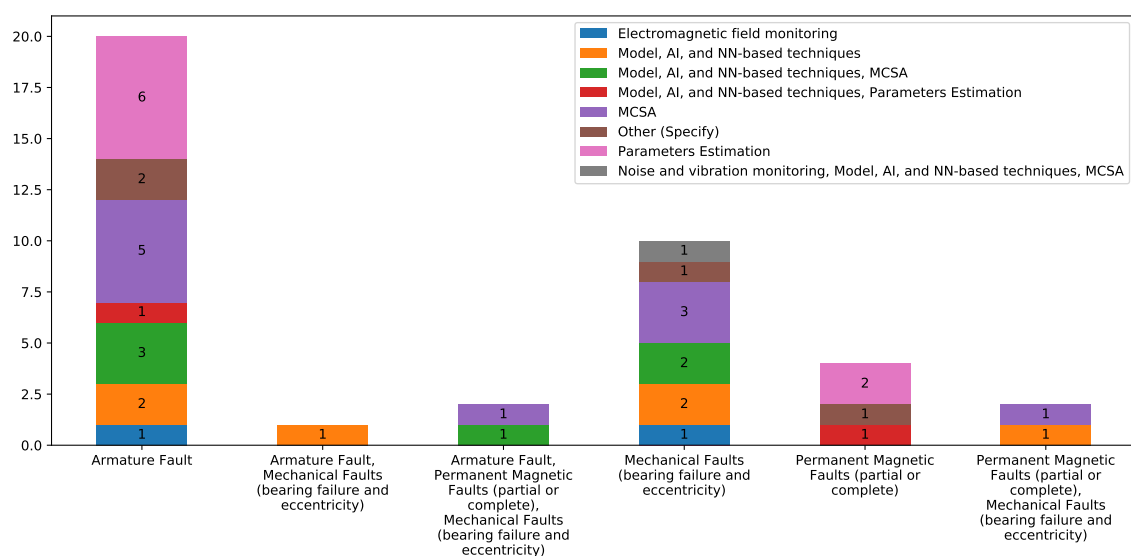

Figure 5. Distribution of the papers according the type of failure and the used technique.

1.1.4. Computational Power Needed for Each Technique

Only a few papers ([11–13]) presented a clear determination of the computational power needed to implement the proposed technique, hence this question can be answered only in a qualitative way. The most computationally demanding techniques are based on models. This because of the need to run the machine model in parallel to the machine itself while comparing the outputs. The complication also grows with the model level of detail, the parameters involved, etc. Then come the techniques based on parameter estimation and those which make use of NNs. In any case much depends on the way the algorithms are implemented.

The least expensive techniques, in terms of computational load, are the MCSA and other techniques which directly analyse sensor data.

1.1.5. Sensors Needed for Each Technique

The quasi-totality of methods need to at least measure the current consumption and the motor voltage, but these quantities are already accessible in the majority of the drivers. Many methods also use the motor speed to correctly diagnose the failure. The speed can either be estimated, for example from the back-EMF measurements, or obtained directly from the Hall effect frequency sensors, or from a resolver. Overall, the techniques which definitely require fewer sensors are those based on current or voltage analysis, such as the MCSA.

1.1.6. Best Detection Results

Only a portion of the selected papers ([8,9,11–18]) clearly show statistics on the fault detection rates and mostly are based on the use of AI.

On the other hand, it is very difficult to compare the results of different techniques due to the fact that the testing conditions are not uniform.

This is considered as a weak point of this topic which, although being very rich in ideas and proposed techniques, lacks in validation and verification of the same. An interesting solution to this issue would be to propose a minimum standard set of tests to be executed to validate a fault detection algorithm.

1.2. General Considerations about the Techniques

Table 3 contains a brief summary with the characteristics of the main methods included in the literature review:

As already said, the techniques based on AI are very powerful. They can be used as standalone fault detectors or in conjunction with other techniques to strongly improve their detection performance. In any case it has to be considered that their effectiveness depends upon an intensive learning phase and they take considerable time before working correctly. It is also inherently difficult to establish a deterministic way of working for them, and this can cause some issues when using them in the aeronautical field where they need to be certified for safety critical tasks.

According to the statistics presented in the previous section, the papers presenting fault detection techniques based on parameter estimation have also experienced a growth in number. These techniques can give continuous access to otherwise unobservable variables as for example the back-EMF or the magnetic flux, facilitating the fault detection task or the definition of more directly observable fault indicators. The possible problem with these techniques is that they depend on assumptions, models and measurement of motor variables whose validity limits and inaccuracies can hamper the fault detection.

A very important point to highlight is the capacity of the algorithm to work while the motor is running in non-steady-state conditions of speed and/or torque. According to the results of the present research, about one third of the selected articles proposes a technique capable of working during non-steady-state conditions and most of them are based on AI, NN and parameters estimation. The need to have the motor in steady-state conditions can be an important limitation if the steady-state

is necessary to measure signals over a period of time, which may be obtainable with large industrial machines working at constant load but rarely so in aeronautic actuators.

Table 3. Techniques summary.

Technique	Advantages	Disadvantages
Noise and Vibration Monitoring	Most suitable method for detecting mechanical faults, as the accelerometers can be placed close to the vibration source	Need to install accelerometers on the motor, measurements can be corrupted by environmental vibrations, difficult to use in non-stationary motor operation
Electromagnetic Field Monitoring	Can directly measure the electromagnetic field inside the motor, does not need complicated algorithm to detect failures, can virtually detect all the motor failures	Need to rewind the stator and to extract as many additional cables as many coils inserted
Motor Current Signature Analysis	Does not need additional sensors, can detect a large variety of failures, is the most used technique	Need to transform the signal in the frequency domain, the motor current depend on the load, cannot be used during non-stationary motor operation
Model and AI based techniques	Can be used during non-stationary motor operation, can be used in conjunction with other techniques	Need extensive training
Parameters Estimation	Can be used during non-stationary motor operation, can virtually monitor every motor parameter	The method needs the knowledge of various motor parameters and on the accuracy of the model, their variation (or incorrectness) can result in poor diagnosis performance

1.3. Objectives of the Research

As a contribution to the current state of the art, the following main objectives of this paper can be summarised as:

1. To provide a study of the current literature on fault detection of BLDC motors. By presenting the papers which expose algorithms closest to being implemented These are selected from the vast literature on this topic according to the criteria stipulated in Tables 1 and 2. This choice has been influenced by the experience of the author when dealing with fault detection papers, which often are oriented towards a more academic audience and do not concentrate so much on implementation. The methodology used in this work to compile the state of the art is still not available widely in the engineering world. From this study, some characteristics needed for the fault detection on electric machine have been listed.

2. To propose a new technique for detection of demagnetisation in BLDC motors. This is considered relevant since statistics extracted from the literature shows that demagnetisation is responsible for about the 20% of BLDC motors failures. The algorithm is based on the dissimilarity between the voltages in the various electric turns of the motor caused by this particular failure. The exposed method presents the advantages of not needing domain transforms or previous knowledge of the detail of the motor (with the exception for the number of pole-pairs). Furthermore, the proposed indicators can rapidly be computed and require only the acquisition of motor phases voltages for a mechanical turn.

3. To confirm the hypotheses about the effect of a demagnetisation with Finite Element Method (FEM) analysis and validate the proposed method to detect demagnetisation with experimental tests on a real motor.

2. Proposed Detection Method

This section introduces the method proposed to detect demagnetisation by analysing the dissimilarity of the phase voltages between the electric turns.

For ease of understanding, the theory is presented with reference to the specific BLDC motor used for the experimental tests. However, hopefully it is clear that the validity of the approach is general. Demagnetisation is modelled by assuming that one of the magnets, located on the rotor, is missing. The motor used in the experiments was a 12 slots, 14 poles BLDC. Figure 6 represents this motor with one of the 14 magnets demagnetised or missing.
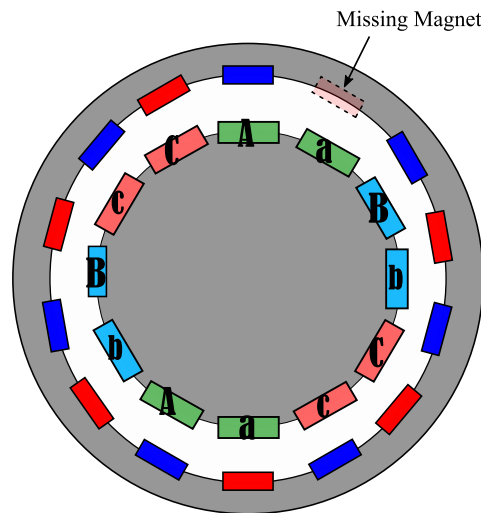

Figure 6. Representation of the used motor with a missing magnet.

The magnetic symmetry of the motor when perturbed, results in the following consequences:

Unbalanced back-EMF throughout one rotor revolution: Even if, for the case of multi-pole, multi-coil motor, the back-EMF change is not so straightforward to imagine, magnet defect causes non-uniformity in the distribution of the air-gap flux, resulting in a reduction of the induced voltage. The decrease in back-EMF translates into an increment of the phase current, due both to the decrease of its own back-EMF or of the alternative phase's back-EMF.

Unbalanced and asymmetrical Magnetic Pull: In a healthy motor the ferromagnetic rotor body is attracted by the magnets with equal strength from every direction. If a magnet is missing, this equilibrium is broken, generating a net pull force in the direction opposed to the missing magnet.

Increased Cogging Torque: In fractional slot motors such as the the one used here, each magnet appears in a different position relative to the stator slots. As a result, the cogging torques created by each magnet is out of phase with the others, therefor the net cogging effect is reduced since the cogging torque from each magnet sums together and at least partially cancels the cogging torque from other magnets [19]. Due to the missing magnet, the distribution of the cogging torque around the physical turn revolution is uneven and, on average, increased.

Abnormal Torque Ripples produced around the mechanical revolution: If the current distribution around the mechanical revolution has its motion perturbed, the produced torque is consequently disturbed, producing abnormal torque ripples around the mechanical revolution. It generates more vibrations and localised accelerations and of the rotor.

Unbalanced Rotor: The rotor itself can be mechanically unbalanced depending if the magnet is missing (partial or total disintegration) or just demagnetised. In the case of a missing magnet there is a strong increase in the vibration level.

In addition, the correct phase switching is disturbed during one electrical turn due to the partial demagnetisation. This effect is variable and depends on the technique used for switching (hall sensors, resolver or sensor-less).

All those effects cause the voltages and currents in the various electrical turns to be different. In this work, the effects will be investigated by means of FEM analysis and experiments. Also, two fault indicators are proposed and compared as a means for fast detection of the partial demagnetisation.

2.1. Fault Indicators

The effects listed in the previous section cause asymmetries between the phase voltages and currents of the electrical turns. Hence a demagnetisation in one pole can be detected by comparing the voltages and currents generated for each electric turn.

This comparison can be carried out with various statistical tools. In this work two indicators will be proposed in order to detect if a motor presents a demagnetisation fault.

The first indicator is named herein I_{xc} and is obtained by extracting the maximum value of the normalised cross-correlation between the electric turns of the motor, i.e.,

$$I_{xc}^{ij} = max \left(\frac{1}{n} \sum_{m=-\infty}^{+\infty} \frac{1}{\sigma_{e_{Ai}}\sigma_{e_{Aj}}} (e_{Ai}^*[m] - \bar{e}_{Ai})(e_{Aj}[m+k] - \bar{e}_{Aj}) \right) \tag{1}$$

with:

i, j = ith and jth electric turn
e_{Ai} = Back-EMF relative to the A phase and ith electric turn

This operation generates a symmetric matrix with dimension depending on the number of pole-pairs pp with ones along the diagonal.

If all the magnets are healthy, the normalised cross-correlation value should be very close to 1. On the other hand, the higher the demagnetisation of one pole, the greater the difference will be in the back-EMF signals and the lower the correlation value.

The same matrix can be built-up for each phase. The three matrices obtained can be averaged or summed. The sum would amplify the correlation difference between the electric turns, but also any possible spurious data. Conversely, by averaging the matrices, both quantities are attenuated. In this work, the sum has been chosen due to the fact that experimental data can be accurately filtered and adjusted before computing the cross-correlation.

The second indicator is the normalised average of the difference between the back-EMF signals of the electric turns. This is indicated by the symbol I_{diff}.

$$I_{diff}^{ij} = \frac{1}{n} \sum_{m=-\infty}^{+\infty} \left| \frac{(e_{Ai} - e_{Aj})}{\|(e_{Ai} - e_{Aj})\|} \right| \tag{2}$$

This indicator should have a value close to zero for a healthy motor and should increase proportionally to the magnet failure entity. The normalisation is executed to reduce the dependence on the motor speed contained in the back-EMF signal.

Also in this case, the indicator generates a symmetric matrix with dimension $pp \times pp$, but with zeros (as a convention, because the norm also would be zero) on the diagonal.

Even in this case, it has been decided to sum the matrices relative to each phase in order to amplify any differences.

Once obtained the two matrices of I_{xc} and I_{diff}, the upper triangular terms of each matrix are summed together to obtain two global indicators, as specified in Formulas (3) and (4):

$$i_{xc} = \sum triu(I_{xc}) \tag{3}$$

and

$$i_{diff} = \sum triu(I_{diff}) \tag{4}$$

2.1.1. Interpretation of Indicator i_{xc}

The closer to unity the normalised correlation is, the more similar the signals. Hence for a healthy motor it is expected that the matrix I_{xc} is filled with values very close to 1, and this is expected also for all the three motor phases. Consequently, the sum of the three I_{xc} matrices shall be a matrix filled with 3. According to Equation (3) the maximum value for the i_{xc} indicator is:

$$i_{xc}^{max} = \frac{(pp - 1) \cdot (pp)}{2} \cdot 3 \tag{5}$$

So for example, a healthy motor with 4 pole-pairs motor should have an ideal value of $i_{xc} = 18$.

2.1.2. Interpretation of Indicator i_{diff}

Similar reasoning can be used for this indicator, but in this case the matrix is expected to be filled with zeroes for an healthy motor. In this case, a healthy motor would have a value of i_{diff} very close to zero, i.e.,

$$i_{diff}^{min} = 0 \tag{6}$$

The graph in Figure 7 summarises how to compute the indicators.

In order to be applied, the proposed technique needs to assume as valid the following statements:

1. Multi-pole Motor ($pp > 1$),
2. Partial demagnetisation (an uniform demagnetisation of all the magnets, although more improbable, would not generate any dissimilarity between the electrical turns)
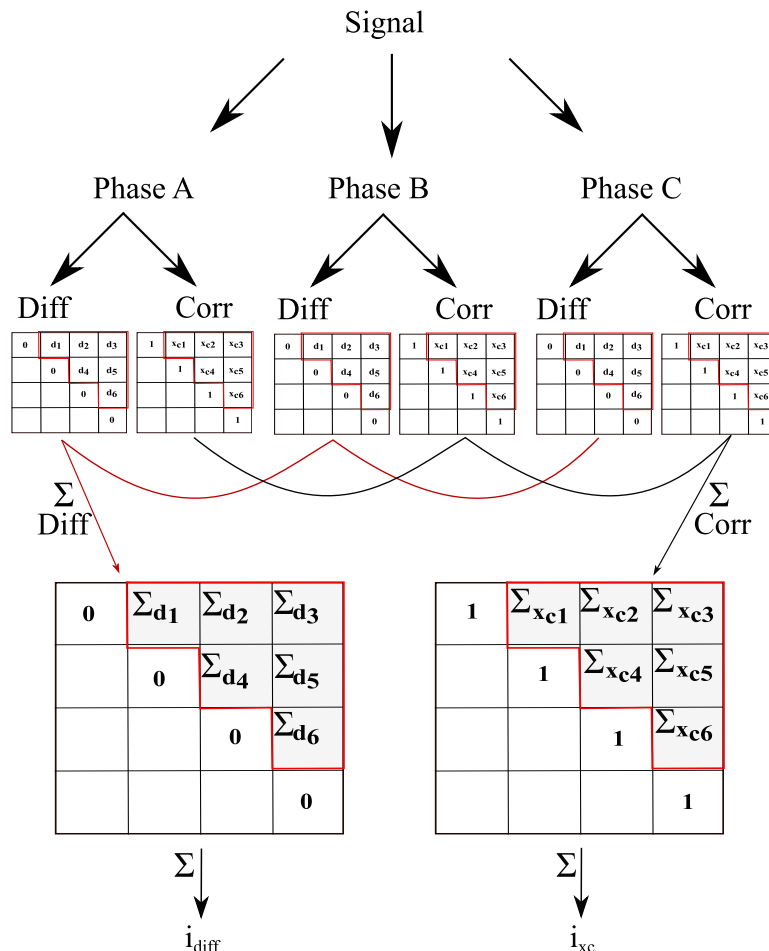

Figure 7. Indicators computation process summary.

3. FEM Analysis

In order to obtain an accurate FEM model, a specimen motor has been completely dismantled. During the procedure, most of the motor data necessary for the modelling have been directly observed.

The basic model of the motor has been realised in the RMxprt package of Ansys Electromagnetic Suite and then exported to Maxwell 2D to perform a transient FEM analysis. Time variation of the stator currents, torque and speed can be calculated, as well as the induced voltages on stator winding.

The model has been modified to simulate a partial motor demagnetisation. The partial demagnetisation has been reproduced by simply changing the magnetic properties of one magnet. In detail, the magnet coercitivity magnitude has been reduced from −560,000 Am to −1000 Am.

Figure 8a displays the magnitude of the magnetic flux established inside the different motor parts, in the nominal condition, while Figure 8b shows the results of the simulation in the case of a damaged magnet. A remarkable flux reduction is clearly visible, corresponding to the damaged magnet and a resulting asymmetry in the magnetic field distribution.

Before the execution of the experimental tests, the simulated data has been computed on the indicators. First, the phase voltages have been simulated for a complete mechanical revolution. Then, they have been split into 7 parts, i.e., the number of motor's polepairs. Each chunk represents a mechanical revolution.

At this point there are 3 groups, one for each phase, containing the phase voltage signals of the 7 electrical revolutions.

(**a**)　　　　　　　　　　　　　　　　　　　　(**b**)
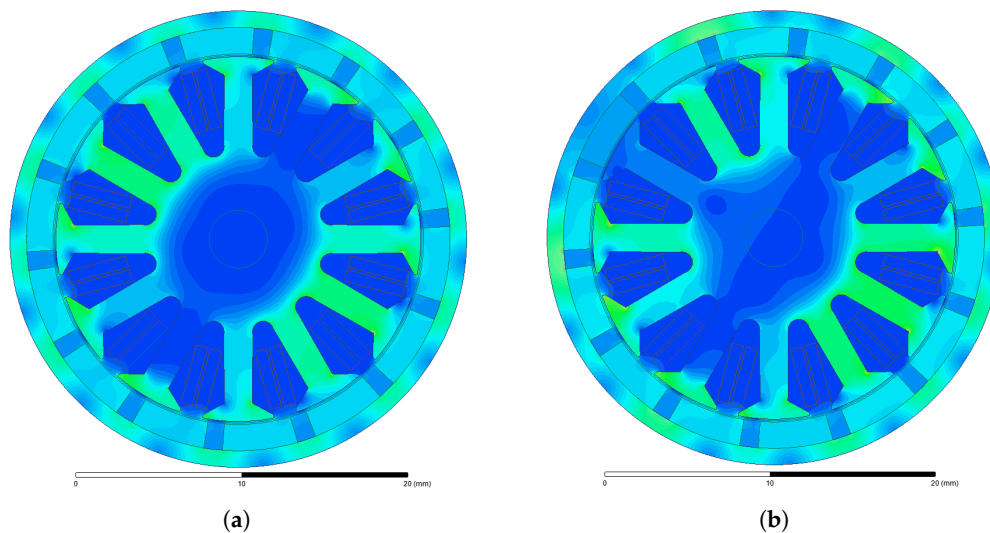
Figure 8. Comparison of Intensity of the Magnetic Flux Density in healthy and damaged motors. (**a**) Intensity of the Magnetic Flux Density in the healthy motor; (**b**) Intensity of the Magnetic Flux Density in the motor with a demagnetised magnet.

By comparing the set of figures in Figure 9, it is possible to observe that, while for the healthy case the phase voltages of the electrical rotations are completely overlapping, for the demagnetised motor they are different during the non-conducting steps.
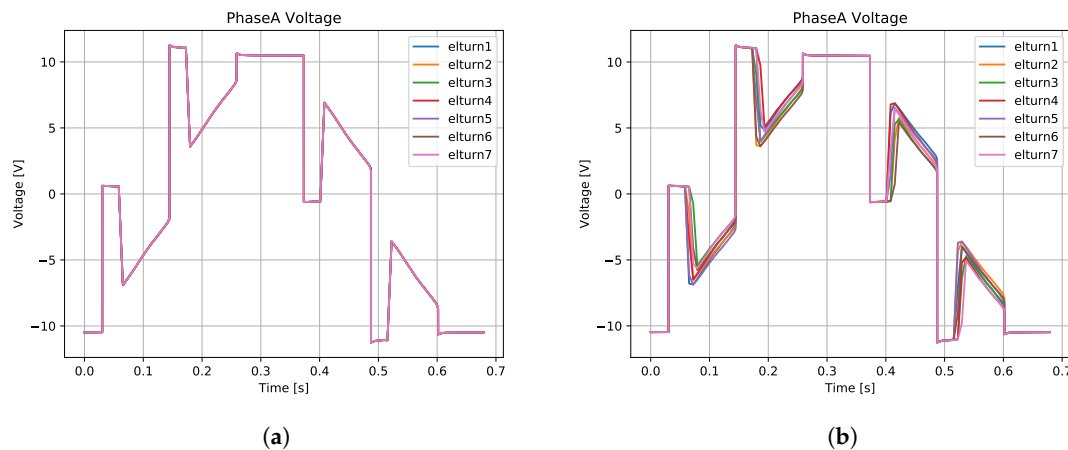
Figure 9. Comparison of the Phase A Voltages of the healthy and damaged motor—12,500 RPM. (**a**) Phase A Voltage—Healthy; (**b**) Phase A Voltage—Damaged.

It is now possible to compute the indicators i_{xc} and i_{diff}, by following the procedure summarised in Figure 7, obtaining the results in Table 4.

Table 4. Indicators computed from simulation data—12,500 RPM.

Indicator	Healthy	Demagnetised	Theoretical Values (Healthy)
i_{xc}	62.99	62.44	63
i_{diff}	2.34	2.42	0

The indicators correctly show that the signals relative to electrical turns of the demagnetised motor are more dissimilar between them. This result will be checked in section with the experimental tests.

4. Experimental Results

The experiments have been carried out by using the P-NUCLEO-IHM001, a development kit composed by a control board, a power board and a brushless motor. The voltage signals have been obtained by measuring with the oscilloscope at the pins corresponding to the signals BEMF1, BEMF2 and BEMF3 of the P-NUCLEO board. The primary role of this circuit is to measure the motor back-EMF, but in this work the entire phase-phase voltage will be acquired and used. The voltage signals are clamped to 3.3 V in order to be directly read by the microcontroller's Analog to Digital Converter (ADC). The motor was fastened to the lab table through the four dedicated fixing screws visible in Figure 10a. The laboratory temperature was maintained between 20–25 Celsius degrees throughout.

4.1. Motor Demagnetisation Procedure

In performing the experiments, the motor was partially demagnetised by removing one of the 14 magnets and replacing it with a block of aluminium of similar weight ($\approx$0.19 g) and size, to avoid the effects of eccentricity caused by the weight unbalance on the rotor. The aluminium was chosen for having a magnetic permeability very similar to the motor magnets. In this way it has been possible to replicate the effect of a complete loss of the magnetic properties without compromising the balance of the rotor.

The magnet was removed by chemically dissolving the glue which connected it to the rotor and due to this procedure, no other parts of the motor were damaged. The result of this process is shown in Figure 10.

(**a**)   (**b**)
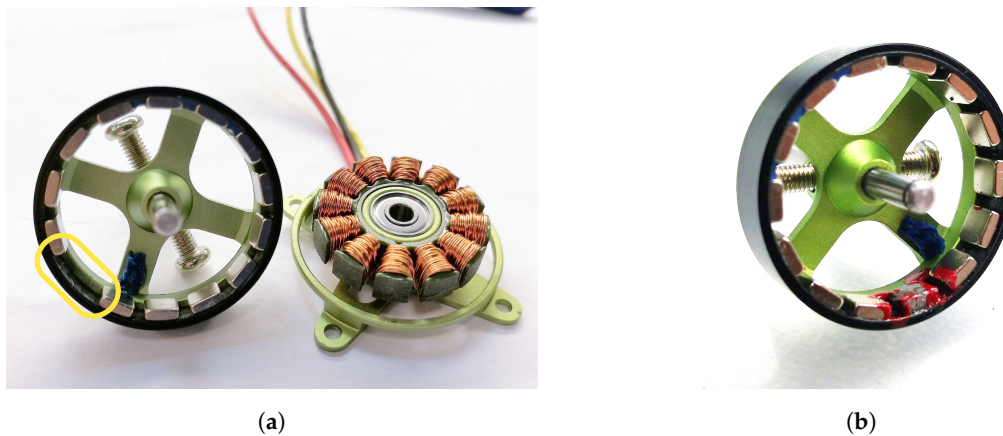
Figure 10. Demagnetisation process: rotor with a missing magnet (**a**), highlighted by the yellow circle, and rotor with the replacement piece of inert material (**b**), easily recognisable for the red glue.

4.2. Data Acquisition

Figure 11a shows the acquisition of about 2 ms of the phase voltage, using an oscilloscope with the motor running at a constant speed of 3000 RPM. From the figure it is possible to observe that the motor is controlled by varying the average voltage with the technique of the Pulse Width Modulation (PWM), and, in order to apply the proposed technique, a low-pass filter needs to be applied.

(**a**)   (**b**)
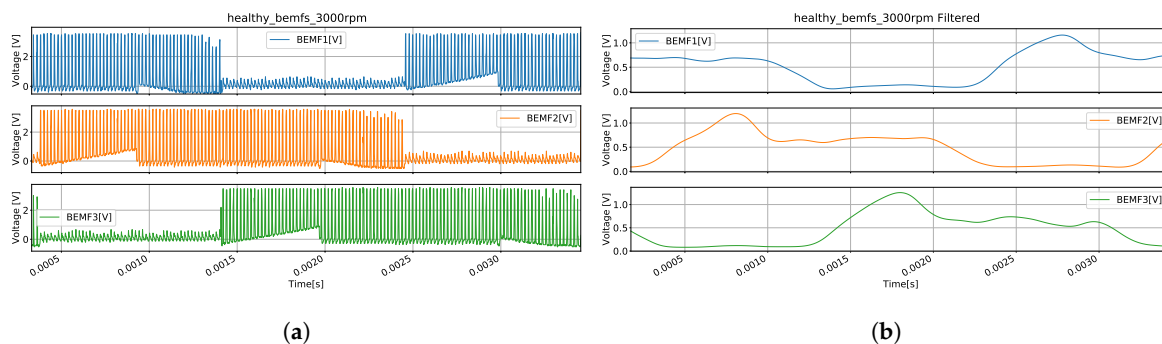
Figure 11. Comparison of the measured phase voltage, before and after the filtering. (**a**) Oscilloscope acquisition—3000 RPM; (**b**) Filtered oscilloscope acquisition—3000 RPM.

These phase-phase voltage signals contain information about both the conduction component and the back-EMF. The flux asymmetry throughout the mechanical revolution, generated by the missing magnet, is expected to be reflected in these phase voltage as a dissimilarity between the electrical turns.

The measured voltage signals are then filtered by a Butterworth low-pass filter with the cut-off frequency set to the current angular speed multiplied by the number of pole-pairs. The signals resulting from filtering the signals in Figure 11a are shown in Figure 11b.

Table 5 summarises the operating conditions, and the relative data, for which data have been measured for both the healthy and the partially demagnetised motor at different speeds. The duration of the acquisition period has been reduced according to the speed, to preserve a similar resolution in the period.

The measurements refer to the same motor, i.e., the first set of voltage measurements were taken on the motor before the demagnetisation procedure. Then the motor was unmounted, the magnet substituted and re-mounted to perform the measurements in the faulty state. This way, the inevitable presence of differences caused by the use of two motors has been avoided.

Table 5. Acquisitions summary.

Speed	Load	Duration	Points	Timestep
3000 RPM	No-Load	0.1 s	65,250	1.53×10^{-6} s
5000 RPM	No-Load	0.1 s	65,250	1.53×10^{-6} s
7000 RPM	No-Load	0.1 s	65,250	1.53×10^{-6} s
9000 RPM	No-Load	0.05 s	65,250	7.66×10^{-7} s
11,000 RPM	No-Load	0.05 s	65,250	7.66×10^{-7} s

4.3. Electrical Cycle Division and Indicators Evaluation

After the acquisition and filtering, the voltage signals are then divided for each electrical cycle and by phase.

Then seven electrical turns are grouped as a mechanical turns. The result of this operation is a collection of mechanical turns, each containing seven electrical turns for each phase. This is the last step before computing the indicators.

The whole procedure is represented in Figure 12.
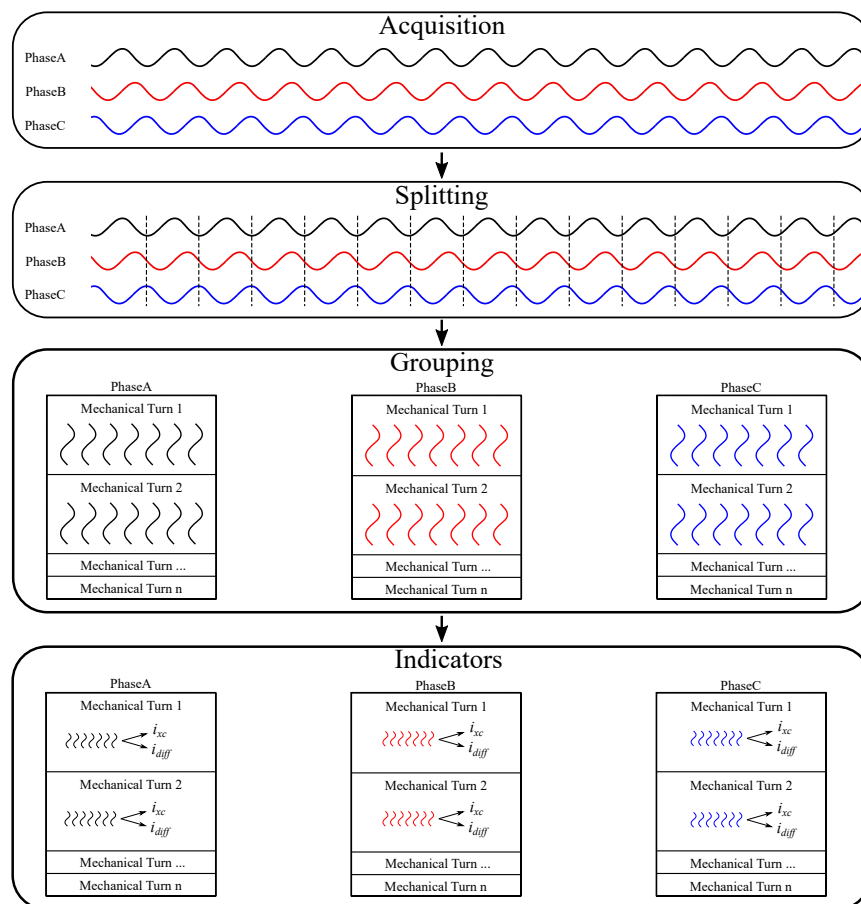
Figure 12. Procedure to obtain the indicators.

Figure 13 shows the result of the electrical cycle splitting and corresponding grouping operations. Each curve represents an electrical turn of the same mechanical revolution and phase, obtained for the healthy and for the demagnetised motor. By comparing the two graphs, it will be noticed that the phase curves of the demagnetised motor are much more dissimilar between them. This dissimilarity is caused by the partial demagnetisation and it will be used to detect the failure. Although this picture refers to a specific motor speed, the same dissimilarity is also observed (with different magnitude) at different motor speeds.
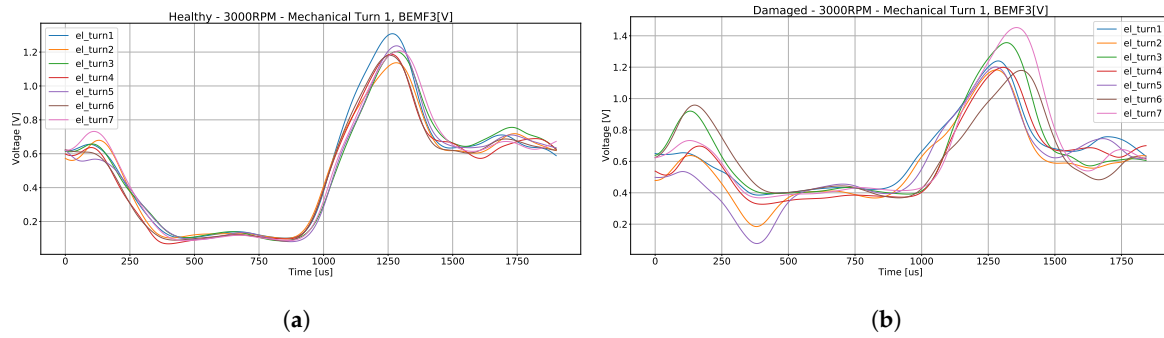
Figure 13. Superposition of the 7 electrical turns relative to the same mechanical turn, of a healthy and damaged motor running at 3000 RPM. (**a**) Healthy motor; (**b**) Damaged motor.

Figure 14 shows instead the same electrical turn compared over various mechanical turn with the motor running at different speeds. For example, in this case the electrical turn no.1 of Phase A and the electrical turn no. 5 of the Phase C have been used, over 4 different mechanical turns with the motor running respectively at 3000 RPM and 9000 RPM. By comparing the healthy and faulty motor, no appreciable differences can be found. This suggests that the dissimilarity seen in Figure 13 is not random, but instead that the flux distribution is repeated for each mechanical turn.
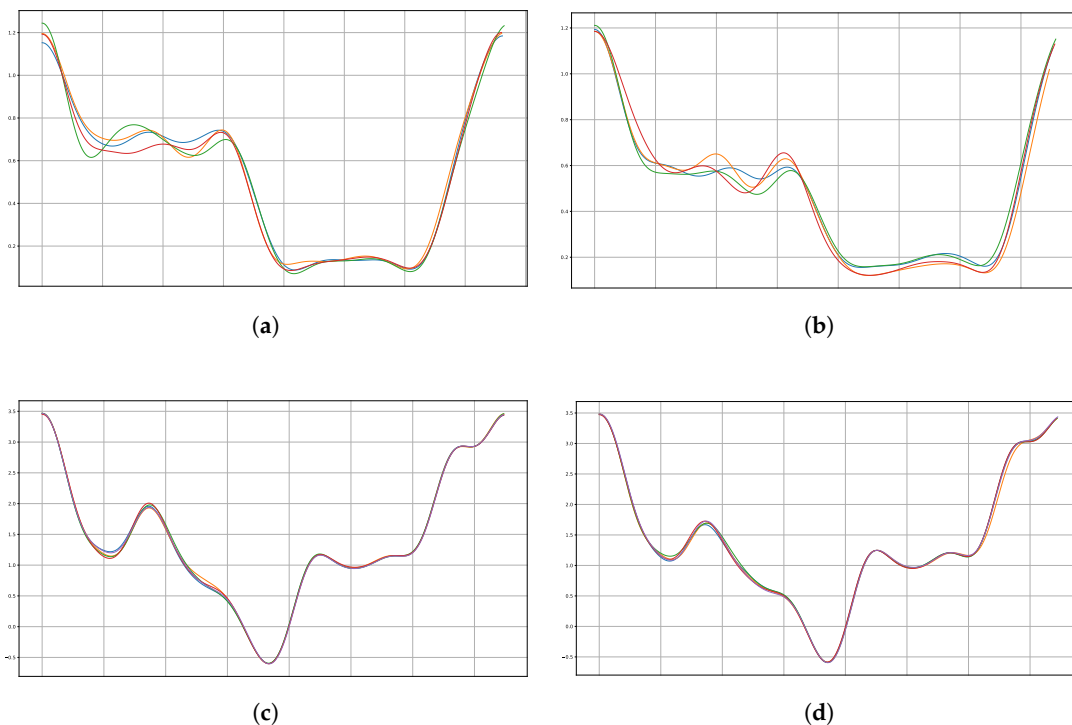
Figure 14. Comparison of the same electrical turn voltage over *4 mechanical turns* for different speeds and phases. (**a**) Phase A—Electrical turn n.1—3000 RPM—healthy motor; (**b**) Phase A—Electrical turn n.1—3000 RPM—partially demagnetised motor; (**c**) Phase C—Electrical turn n.5—9000 RPM—healthy motor; (**d**) Phase C—Electrical turn n.5—9000 RPM—partially demagnetised motor.

4.4. Results—Steady State Conditions

In this section, the indicators values obtained for various speeds will be shown, for both the healthy and faulty motor with the motor running in steady state conditions. Furthermore the performance of the two proposed indicators will be explained, determining which of the two is best suited for fault detection.

4.4.1. Cross-Correlation Indicator

Figure 15 shows various graphs containing the i_{xc} indicator calculated at different speeds, for the healthy and demagnetised motors. The graph has been generated by using four consecutive mechanical turns for each speed, in order to show the evolution of the coefficients over various turns.

As expected by considering the plots of Figure 13, the value of correlation is higher for the healthy motor, and, as predicted, it is very close to the theoretical value that can be computed with Formula (5), i.e.,

$$i_{xc}^{max} = \frac{(7-1) \times (7)}{2} \times 3 = 63 \tag{7}$$

(a)　　　　　　　　　　　　　　　　　　　　(b)

(c)　　　　　　　　　　　　　　　　　　　　(d)

(e)
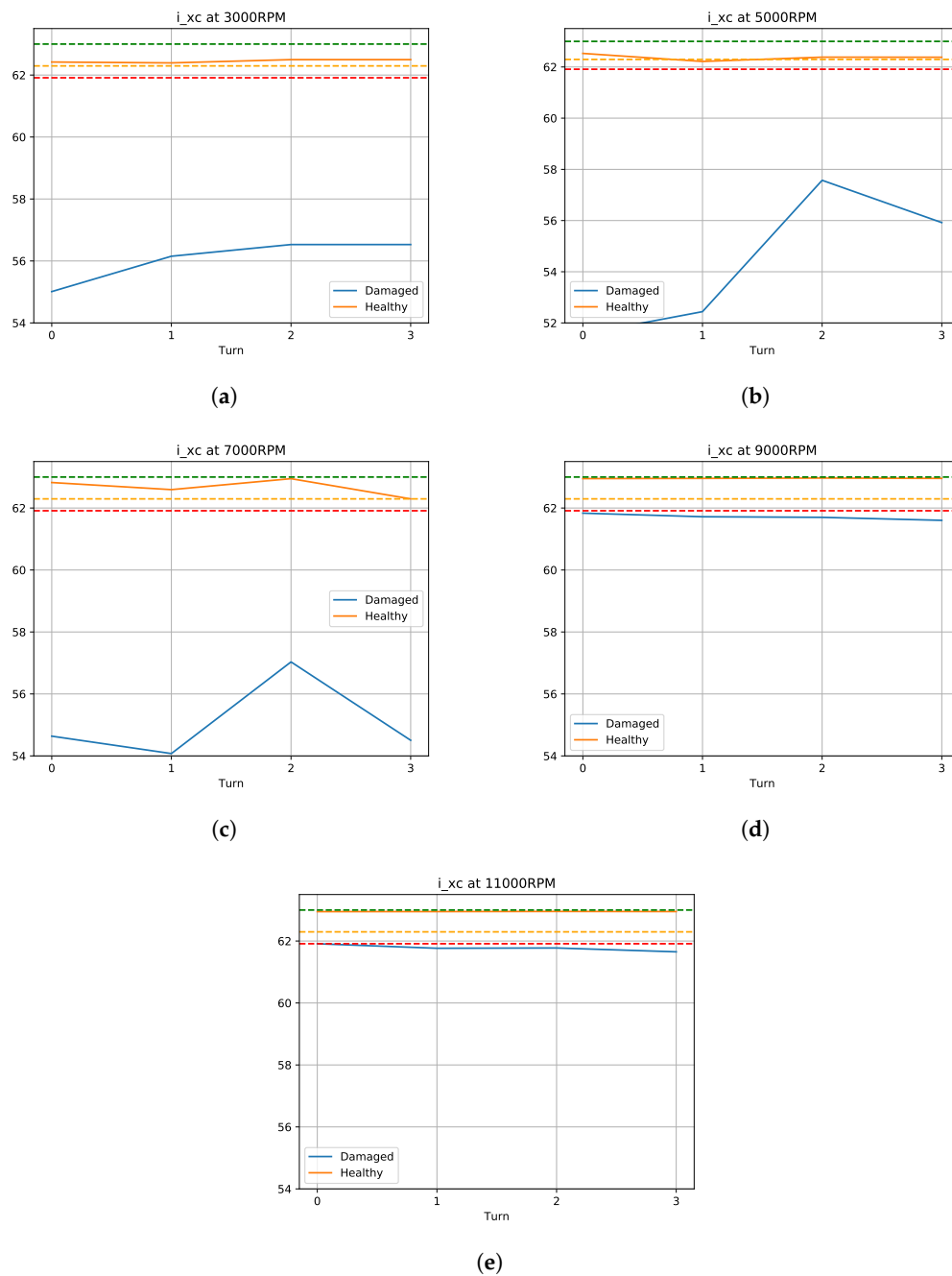
Figure 15. i_{xc} indicator at various speed for healthy and faulty motors. (**a**) i_{xc}—3000 RPM; (**b**) i_{xc}—5000 RPM; (**c**) i_{xc}—7000 RPM; (**d**) i_{xc}—9000 RPM; (**e**) i_{xc}—11,000 RPM.

Two important aspects to consider when dealing with fault indicators appear from the graph:

Separation There is a good separation over all the mechanical turns between the indicators corresponding to the healthy and to the demagnetised motor. In order to show this, in Figure 15, two dashed lines have been included, one in orange and one in red, representing respectively the minimum i_{xc} value for all the acquisitions of the healthy motor and the maximum i_{xc} value for all the acquisitions of the damaged motor. It can be seen that the boundaries are never exceeded for any speed.

Consistency The indicators are consistent over the mechanical turns, i.e., there are no big oscillations of the indicators. Above all the indicators relative to the healthy motor appear to be extremely stable, also at different speeds. The maximum measured variation of i_{xc} for the healthy motor has been 1.11% with reference to the theoretical value of 63, while on average it varies only by 0.38%.

On the other hand, the i_{xc} of the demagnetised motor varies largely according to the speed, reducing the separation at higher values of angular velocity. This effect can be seen also (with a reduced intensity) in the healthy motor and is probably due to the higher angular momentum of the rotor which better compensates for the torque unbalance effects. Anyway this does not represent an obstacle to the fault detection as the indicator values are still separated as can be seen from Figure 15.

The definition of the maximum theoretical value of the indicator is also an important characteristic of i_{xc} indicator; indeed it also permits the evaluation the behaviour of the healthy motor.

4.4.2. Normalised Averaged Difference Indicator

In Figure 16 various graphs containing the i_{diff} indicator calculated at various speeds are shown, for the healthy and demagnetised motor and for several mechanical turns.
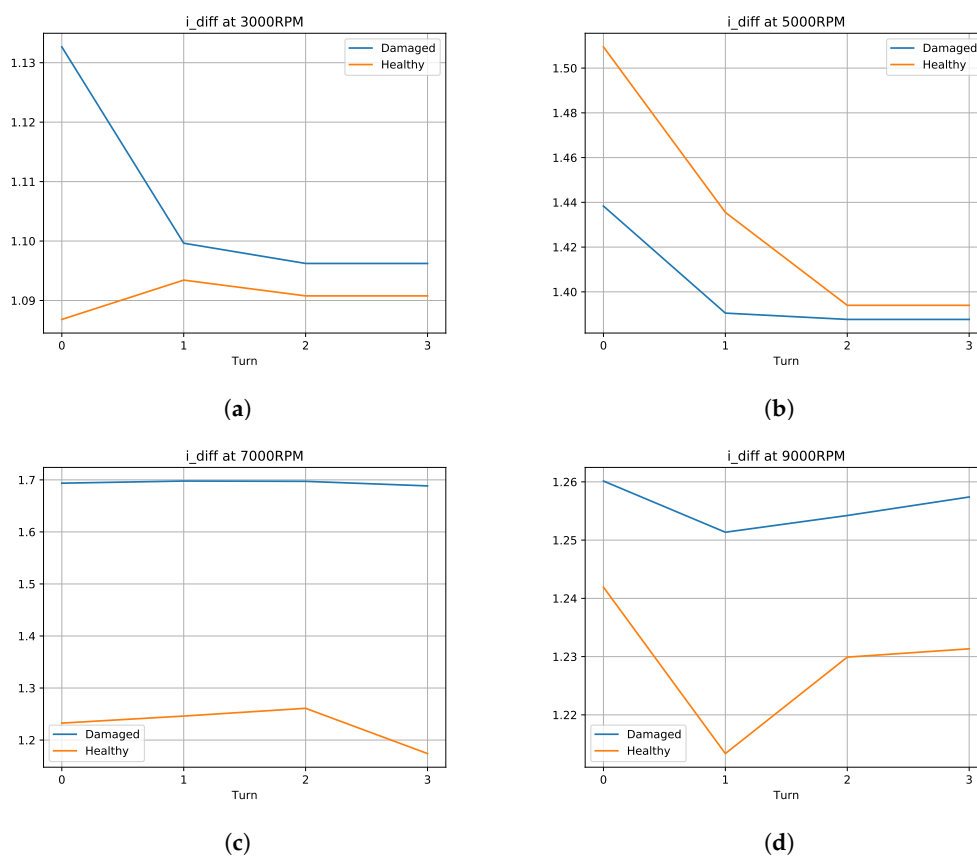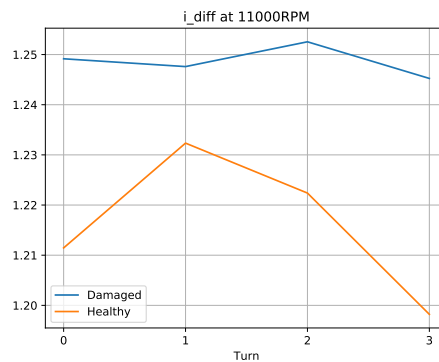

(a)

(b)

(c)

(d)

Figure 16. *Cont.*

(**e**)

Figure 16. i_{diff} indicator at various speed for healthy and faulty motors. (**a**) i_{diff}—3000 RPM; (**b**) i_{diff}—5000 RPM; (**c**) i_{diff}—7000 RPM; (**d**) i_{diff}—9000 RPM; (**e**) i_{diff}—11,000 RPM.

In this case, even if the indicators i_{diff} of the healthy and demagnetised motor are still separated, it cannot be said that they present consistency and a good separation. The indicators appear to be more unstable and they move in a much smaller interval, which makes it difficult to distinguish between healthy and demagnetised. Also, the indicators values strongly depend on motor speed, with an erroneous evaluation at 5000 RPM, which does not allow drawing the same thresholds as for the indicator i_{xc}. Anyway, this indicator can still be useful if used as a confirmation or with some type of automatic classifier like a NN or an algorithm based on Support Vector Machines (SVMs).

4.5. Possible Use of the Indicators

Given the characteristics of the indicator i_{xc}, it appears well suited both for continuous monitoring and for occasional health testing of the motor. Given the high consistency of i_{xc} for a healthy motor, a threshold can be easily established in order to determine as faulty those motors for which i_{xc} falls below this limit.

In this case for example, the two limits proposed in Figure 15 can be used respectively as warning and alarm thresholds. Indeed, for the current experiment, the motor can be considered healthy if the indicator stays between the green and orange dashed lines, or to be kept under constant monitoring if it stays between the orange and red dashed lines, and faulty if it goes beneath the red dashed line. Furthermore the separation increases when the motor is running at lower speed.

Another option that can be used for motors performing critical tasks, is to use both indicators in conjunction with a classifier, in order to improve the fault detection task. This enhancement comes at the cost of an increased computational burden and by adding a time consuming step such as algorithm training.

4.6. Execution Time

The average computation time of i_{xc} and i_{diff} is $\approx$4 ms for both, with an algorithm implemented in Python run on a PC with a I5 7200U processor (2.5 GHz).

4.7. Results—Non-Steady State Conditions

In order to assess the performance of the i_{xc} indicator during speed changes, various experiments have been executed. With the motor running at a fixed speed, a step command was sent to the motor to increase the speed in increments of 1000 RPM.

Table 6 summarises the tests executed at variable speed.

Table 6. Variable Speed Acquisitions summary.

Speed1	Speed2	Load	Duration	Points	Timestep
3000 RPM	4000 RPM	No-Load	0.1 s	65,250	1.53×10^{-6} s
5000 RPM	6000 RPM	No-Load	0.1 s	65,250	1.53×10^{-6} s
7000 RPM	8000 RPM	No-Load	0.1 s	65,250	1.53×10^{-6} s
9000 RPM	10,000 RPM	No-Load	0.05 s	65,250	7.66×10^{-7} s

Figure 17 shows the i_{xc} indicator computed during the tests of Table 6. With reference to Section 4.4.1 it can be observed that:

Separation The separation between the healthy and damaged motor indicators is still present, even if it is no longer possible to draw a static threshold between the lines

Consistency For the variable speed tests the consistency of the i_{xc} indicator is somewhat lost; indeed it is also possible to observe non negligible variations of the indicator in the healthy case.

(a)

(b)

(c)

(d)
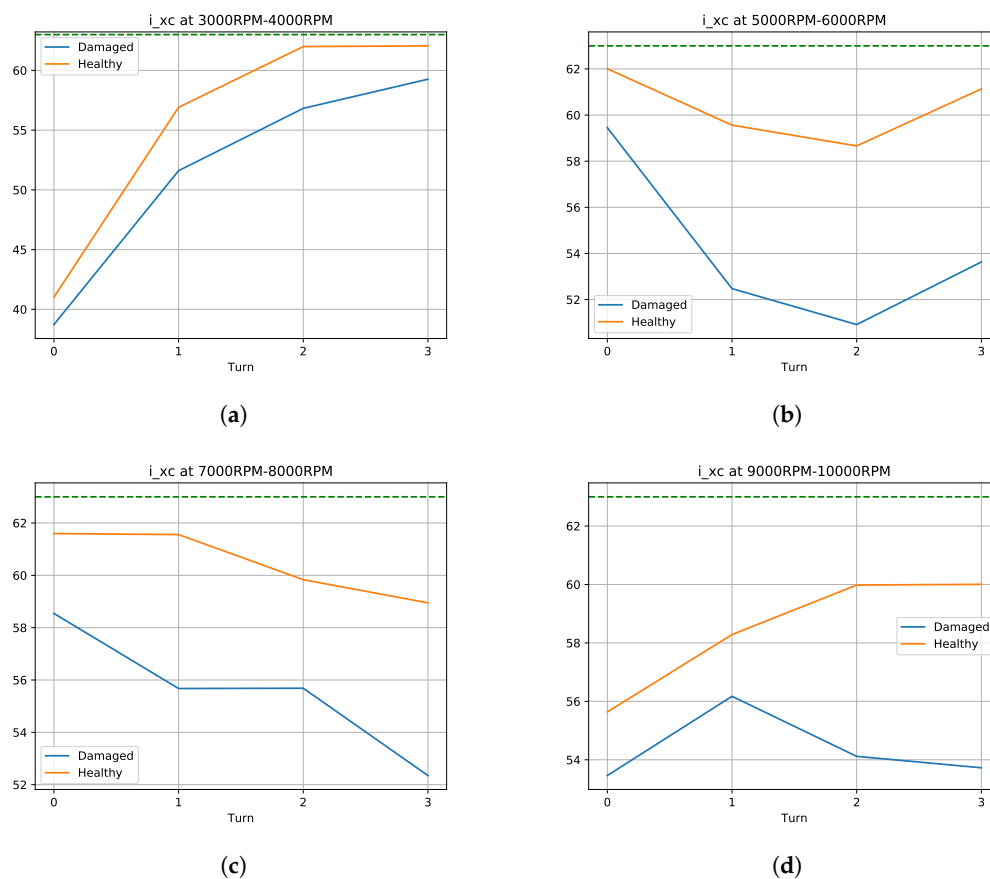
Figure 17. i_{xc} indicator behaviour during speed variation for healthy and faulty motors. (**a**) i_{xc}—3000 RPM–4000 RPM; (**b**) i_{xc}—5000 RPM–6000 RPM; (**c**) i_{xc}—7000 RPM–8000 RPM; (**d**) i_{xc}—9000 RPM–10,000 RPM.

Possible Use of the Indicator

In case of speed variation during the mechanical turn, it is not possible to set a static threshold to detect a failure. On the other hand, the indicators relative to a healthy and a faulty motor are still well separated and it would be possible to repeat it with a classification algorithm.

5. Discussion

A fault detection algorithm based on similarity measurement between the electrical turns corresponding to the same mechanical turn has been elaborated according to the criteria of Table 1. By analysing the indicator performance with experimental tests at various speed, the results seem promising, primarily for what concerns the indicator i_{xc} which presents good consistency over a wide range of speeds. Further characteristics of the same are given in the next sections.

5.1. Applications and Limitations

The indicators have been studied, simulated and experimented with only on a BLDC motor. In any case it is not excluded that, with some adaptation, they could be used on different types of motors; indeed this can be an argument for a future work.

Another important consideration is that, in order to detect demagnetisation, the motor should have several pole pairs greater than 2. This because the algorithm makes comparison between the electric turns and it is therefor necessary to have more than one. Another characteristic is that it can only detect partial demagnetisation. The demagnetisation of all the magnets to the same level, although very improbable, would not cause those differences in the voltage signals needed for fault detection.

Various tests have been executed both at fixed and variable speed. In the first case it was possible to define a threshold to discern between the healthy and the demagnetised motor, while in the second case, even if the indicators are still separated, it was not possible to define a fixed threshold. Hence, if no classification algorithms are used (SVM, NN, AI, etc.), the indicator should be computed when the motor is running in steady state conditions.

5.2. Advantages

The method of fault detection by using the proposed indicators has the main advantage of being straightforwardly applicable with no need for extra hardware. The main technical advantage is the simplicity, regarding both the theoretical formulation and the algorithm implementation, which leads to a high execution speed and low computational burden. Its simplicity is also valuable from the economical point of view, requiring a short implementation time and a few hardware resources, while providing a valuable failure detection tool. Another important characteristic to be highlighted is that the only previous knowledge needed of the motor is the number of pole-pairs. Also the intermediate data are easy to understand as they represent physical variables of the motor in the time domain. Also, due to to this, no domain transformations for frequency analysis are needed, saving computation time.

The algorithm to compute the indicators is composed of a few simple steps and is fast to execute. Indeed the execution time for the PC implementation is already very low and an optimised implementation in a lower level programming language could easily fit in a microcontroller and be executed at even higher speed, permitting both real time monitoring and punctual testing during maintenance.

Having a theoretical value for the indicator is also an important advantage, because it permits the evaluation of a motor without previous knowledge of the same; indeed a healthy motor should have an i_{xc} value always very close to the maximum computed with the Formula (5).

Finally, although it is true that constant speed is required for a correct analysis, it is necessary for just one mechanical turn, i.e., for a few milliseconds. For example if the motor is running at 3000 RPM, a complete turn is executed in 20 ms.

5.3. Future Works

The technique presented has demonstrated promising performance and fault detection capabilities. In the near future, more experimental tests will be executed in order to extend the algorithm's applications. More in detail:

- Experimental tests on BLDC motors with a different number of polepairs, geometry and power
- Tests with different load conditions
- Experimental tests with different types of failures

On this last point, it is necessary to say some more. When considering failures other than demagnetisation, two possible scenarios appear:

1. Other failures have no influence on the proposed method,
2. Other failures have influence on the proposed method.

In the first scenario the proposed method would detect and diagnose demagnetisation.

In the second scenario the proposed method would detect different failures but diagnosis must be performed by further steps or techniques.

Another hint for a future work arose from the study of the state of the art, i.e., the standardisation of the tests to be executed to assess the performance of the fault detection algorithms. Indeed one difficulty encountered during the study of the state of the art has been the impossibility of comparing the performance of the different proposed algorithms, due to the non-uniformity in tests, measured characteristics and presentation of the results. A possible solution to this issue could be the introduction of a standardised benchmark and a set of parameters to be presented in order to harmonise the evaluation of the fault detection algorithms.

Abbreviations

The following abbreviations are used in this manuscript:

AI	Artificial Intelligence
BLDC	Brushless Direct Current
EMA	Electro-Mechanical Actuator
EMF	ElectroMotive Force
FEM	Finite Element Method
HF	High Frequency
MCSA	Motor Current Signature Analysis
NN	Neural Network
PWM	Pulse Width Modulation
SLR	Systematic Literature Review
SVM	Support Vector Machine
TRL	Technology Readiness Level

References

1. Basak, D.; Tiwari, A.; Das, S.P. Fault diagnosis and condition monitoring of electrical machines—A review. In Proceedings of the IEEE International Conference on Industrial Technology, Mumbai, India, 15–17 December 2006; pp. 3061–3066. [CrossRef]
2. Bellini, A.; Filippetti, F.; Tassoni, C.; Capolino, G.A. Advances in Diagnostic Techniques for Induction Machines. *IEEE Trans. Ind. Electron.* **2008**, *55*, 4109–4126. [CrossRef]
3. Kitchenham, B.; Charters, S. *Guidelines for Performing Systematic Literature Reviews in Software Engineering*; EBSE Technical Report; Elsevier: Amsterdam, The Netherlands, 2007; pp. 1–65.

4. Ierardi, C.; Orihuela, L.; Jurado, I. Guidelines for a systematic review in systems and automatic engineering. Case study: Distributed estimation techniques for cyber-physical systems. In Proceedings of the European Control Conference, Limassol, Cyprus, 12–15 June 2018; pp. 2230–2235.

5. Arellano-Padilla, J.; Sumner, M.; Gerada, C. Winding condition monitoring scheme for a permanent magnet machine using high-frequency injection. *IET Electr. Power Appl.* **2011**, *5*, 89–99.

6. Park, Y.; Fernandez, D.; Lee, S.B.; Hyun, D.; Jeong, M.; Kommuri, S.K.; Cho, C.; Reigosa, D.; Briz, F. On-line detection of rotor eccentricity for PMSMs based on hall-effect field sensor measurements. In Proceedings of the 2017 IEEE Energy Conversion Congress and Exposition (ECCE), Cincinnati, OH, USA, 1–5 October 2017; pp. 4678–4685.

7. Nandi, S.; Toliyat, H.A.; Li, X. Condition monitoring and fault diagnosis of electrical motors—A review. *IEEE Trans. Energy Convers.* **2005**, *20*, 719–729. [CrossRef]

8. Abed, W.; Sharma, S.; Sutton, R.; Motwani, A. A robust bearing fault detection and diagnosis technique for brushless DC motors under non-stationary operating conditions. *Control Autom. Electr. Syst.* **2015**, *26*, 241–254. [CrossRef]

9. Çira, F.; Arkan, M.; Gümüş, B. A new approach to detect stator fault in permanent magnet synchronous motors. In Proceedings of the 2015 IEEE 10th International Symposium on Diagnostics for Electrical Machines, Power Electronics and Drives (SDEMPED), Guarda, Portugal, 1–4 September 2015; pp. 316–321.

10. Nyanteh, Y.D.; Srivastava, S.K.; Edrington, C.S.; Cartes, D.A. Application of artificial intelligence to stator winding fault diagnosis in Permanent Magnet Synchronous Machines. *Electr. Power Syst. Res.* **2013**, *103*, 201–213. [CrossRef]

11. Breuneval, R.; Clerc, G.; Nahid-Mobarakeh, B.; Mansouri, B. Hybrid diagnosis of intern-turn short-circuit for aircraft applications using SVM-MBF. In Proceedings of the 2017 IEEE International Conference on Fuzzy Systems (FUZZ-IEEE), Naples, Italy, 9–12 July 2017; pp. 1–6.

12. Heydarzadeh, M.; Zafarani, M.; Akin, B.; Nourani, M. Automatic fault diagnosis in PMSM using adaptive filtering and wavelet transform. In Proceedings of the 2017 IEEE International Electric Machines and Drives Conference (IEMDC), Miami, FL, USA, 21–24 May 2017; pp. 1–7.

13. Heydarzadeh, M.; Zafarani, M.; Ugur, E.; Akin, B.; Nourani, M. A model-based signal processing method for fault diagnosis in PMSM machine. In Proceedings of the 2017 IEEE Energy Conversion Congress and Exposition (ECCE), Cincinnati, OH, USA, 1–5 October 2017; pp. 3160–3164.

14. Akar, M.; Hekim, M.; Orhan, U. Mechanical fault detection in permanent magnet synchronous motors using equal width discretization-based probability distribution and a neural network model. *Electr. Eng. Comput. Sci.* **2015**, *23*, 813–823. [CrossRef]

15. Ebrahimi, B.M.; Faiz, J. Feature extraction for short-circuit fault detection in permanent-magnet synchronous motors using stator-current monitoring. *IEEE Trans. Power Electron.* **2010**, *25*, 2673–2682. [CrossRef]

16. Haddad, R.Z.; Strangas, E.G. Fault detection and classification in permanent magnet synchronous machines using Fast Fourier Transform and Linear Discriminant Analysis. In Proceedings of the 2013 9th IEEE International Symposium on Diagnostics for Electric Machines, Power Electronics and Drives (SDEMPED), Valencia, Spain, 27–30 August 2013; pp. 99–104.

17. Mbo'o, C.P.; Hameyer, K. Fault diagnosis of bearing damage by means of the linear discriminant analysis of stator current features from the frequency selection. *IEEE Trans. Ind. Appl.* **2016**, *52*, 3861–3868. [CrossRef]

18. Ondel, O.; Boutleux, E.; Clerc, G. Diagnosis by pattern recognition for PMSM used in more electric aircraft. In Proceedings of the IECON 2011—37th Annual Conference on IEEE Industrial Electronics Society, Melbourne, Australia, 7–10 November 2011; pp. 3452–3458.

19. Hanselman, D.C. *Brushless Permanent Magnet Motor Design*; Magna Physics Pub: Lebanon, OH, USA, 2006; p. 392.